Electrical Engineering Faculty Publications   Department of Electrical Engineering

11-20-2011

Circular and near-circular polarization states of evanescent monochromatic light fields in total internal reflection

R. M. A Azzam
University of New Orleans, razzam@uno.edu

Recommended Citation
R. M. A. Azzam, "Circular and near-circular polarization states of evanescent monochromatic light fields in total internal reflection," Appl. Opt. 50, 6272-6276 (2011).

Circular and near-circular polarization states of evanescent monochromatic light fields in total internal reflection

R. M. A. Azzam

Department of Electrical Engineering, University of New Orleans, New Orleans,
Louisiana 70148, USA (razzam@uno.edu)

Conditions for the production of near-circular polarization states of the evanescent field present in the rarer medium in total internal reflection of incident monochromatic p-polarized light at a dielectric–dielectric planar interface are determined. Such conditions are satisfied if high-index (>3.2) transparent prism materials (e.g., GaP and Ge) are used at angles of incidence well above the critical angle but sufficiently below grazing incidence. Furthermore, elliptical polarization of incident light with nonzero p and s components can be tailored to cause circular polarization of the resultant tangential electric field in the plane of the interface or circular polarization of the transverse electric field in a plane normal to the direction of propagation of the evanescent wave. Such polarization control of the evanescent field is significant, e.g., in the fluorescent excitation of molecules adsorbed at solid–liquid and solid–gas interfaces by total internal reflection. © 2011 Optical Society of America

OCIS codes: 240.0240, 240.6690, 260.0260, 260.5430, 260.6970.

1. Introduction

Total internal reflection (TIR) of an incident monochromatic plane wave of arbitrary polarization state (with nonzero p and s components present) at the planar interface between two transparent media generates an evanescent field in the rarer medium whose state of polarization is in general elliptical and three-dimensional [1–4]. In this paper, we consider conditions that lead to circular or near-circular polarization of the evanescent refracted wave. The transparent media of incidence and refraction of refractive indices n_0 and n_1 are assumed to be linear, homogeneous, optically isotropic, and nonmagnetic. The $e^{j\omega t}$ time dependence, Nebraska–Muller conventions [5,6], and the xyz coordinate system shown in Fig. 1 are adopted.

The 3×1 generalized Jones vectors of the incident (i) and evanescent (e) refracted waves are written as

$$E_i = [\,E_{ix} \quad E_{iy} \quad E_{iz}\,]^t$$
$$= [\,(\sin\phi)E_{ip} \quad E_{is} \quad (-\cos\phi)E_{ip}\,]^t, \qquad (1)$$

$$E_e = [\,E_{ex} \quad E_{ey} \quad E_{ez}\,]^t, \qquad (2)$$

where t indicates the transpose. In Eq. (1), E_{ip} and E_{is} are phasors that represent the time-harmonic p and s components of the incident electric field and ϕ is the angle of incidence that exceeds the critical angle of TIR, $\phi > \phi_c = \sin^{-1}(n_1/n_0)$. Application of boundary conditions to the normal (x) and tangential (y and z) components of the electric field at the dielectric–dielectric interface leads to the following relations between the Cartesian components of the evanescent and incident fields:

$$E_{ex} = T_{11}E_{ix}, \qquad E_{ey} = T_{22}E_{iy}, \qquad E_{ez} = T_{33}E_{iz},$$
$$(3)$$

$$T_{11} = N^2(1 + r_p),$$
$$T_{22} = (1 + r_s),$$
$$T_{33} = (1 - r_p). \tag{4}$$

In Eqs. (4), $N = n_0/n_1$ is the high-to-low refractive index ratio of the two dielectrics, and r_p, r_s are the TIR interface Fresnel coefficients that are pure phase factors:

$$r_p = \exp(j\delta_p), \qquad r_s = \exp(j\delta_s). \tag{5}$$

The TIR phase shifts δ_p, δ_s are functions of N, ϕ given by [7]

$$\tan(\delta_p/2) = N \sec\phi(N^2 \sin^2\phi - 1)^{1/2},$$
$$\tan(\delta_s/2) = N^{-1} \sec\phi(N^2 \sin^2\phi - 1)^{1/2}. \tag{6}$$

The rest of the paper proceeds as follows: In Section 2, incident p-polarized light ($E_{is} = 0$) is assumed; such light produces elliptical polarization of the evanescent refracted field in the xz plane of incidence (plane of the page in Fig. 1) [1,8]. We show that near-circular polarization is achieved at sufficiently large but realistic values of N, ϕ. In Section 3, the incident polarization state $\chi_i = E_{is}/E_{ip}$ that causes circular polarization of the resultant of the y and z tangential components of the electric field in the plane boundary is determined. In Section 4, the incident polarization state $\chi_i = E_{is}/E_{ip}$ that causes circular polarization of the combined x and y transverse components of the electric field of the evanescent wave propagating in the z direction is also obtained. Polarization control of the evanescent field is important in studies of fluorescent excitation of molecules adsorbed at solid–liquid and solid–gas interfaces using TIR [8–10]. Finally, Section 5 gives a brief summary of this work.

2. Near-Circular Polarization of the Evanescent Field Generated by Incident *p*-Polarized Light

The state of polarization of the evanescent refracted field generated by incident p-polarized ($E_{is} = 0$) light is defined by the complex ratio [6]
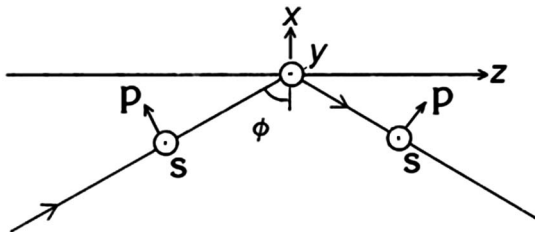
$$\chi_e = E_{ez}/E_{ex}. \tag{7}$$

Fig. 1. Total internal reflection of p- and s-polarized light at a dielectric–dielectric interface at angle of incidence ϕ and the reference xyz coordinate system used to describe the incident and evanescent refracted wave fields.

From Eqs. (1)–(4) and (7),

$$\chi_e = (\cot\phi/N^2)[(r_p - 1)/(r_p + 1)] \tag{8}$$

is obtained. With $r_p = \exp(j\delta_p)$, Eq. (8) simplifies to

$$\chi_e = (\cot\phi/N^2)[j\tan(\delta_p/2)]. \tag{9}$$

Substitution of $\tan(\delta_p/2)$ from Eqs. (6) in Eq. (9) leads to the simple result

$$\chi_e = jb/a = je = j[1 - (\csc\phi/N)^2]^{1/2}. \tag{10}$$

χ_e of Eq. (10) describes an ellipse of polarization with semimajor and semiminor axes a and b aligned with the x and z axes, respectively, and with ellipticity $e = b/a$. In Appendix A we provide an alternate derivation of Eq. (10), which is based on Gauss's law $\nabla \cdot \vec{E}_e = 0$.

Near-circular polarization is achieved if $e = b/a \geq 0.95$. For illustration, Fig. 2 shows a circular state (CS) and an elliptical near-circular state (ENCS) that correspond to $e = 1$ and $e = 0.95$, respectively.

Figure 3 shows $e = b/a$ of Eq. (10) plotted as a function of ϕ from the critical angle $\phi = \phi_c = \arcsin(1/N)$ to grazing incidence $\phi = 90°$ at constant values of the index ratio N from 2 to 6 in steps of 1. Note that $e = 0$, which represents linear polarization in the x direction, occurs at the critical angle ϕ_c and that e asymptotically reaches maximum saturation value

$$e_{\max} = [1 - (1/N)^2]^{1/2} = \cos\phi_c \tag{11}$$

at $\phi = 90°$. The value of N required to achieve a certain $e_{\max}$ is readily obtained from Eq. (11) as
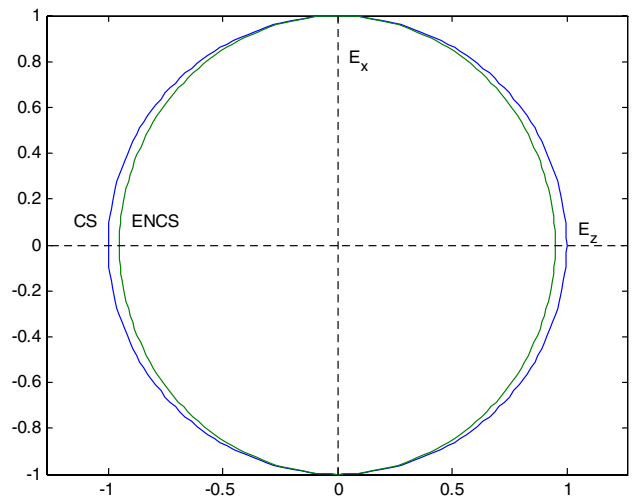
$$N = 1/\sqrt{1 - e_{\max}^2}. \tag{12}$$

Fig. 2. (Color online) Circular polarization state (CS, $e = 1$) and an elliptical near-circular state (ENCS) with $e = b/a = 0.95$.
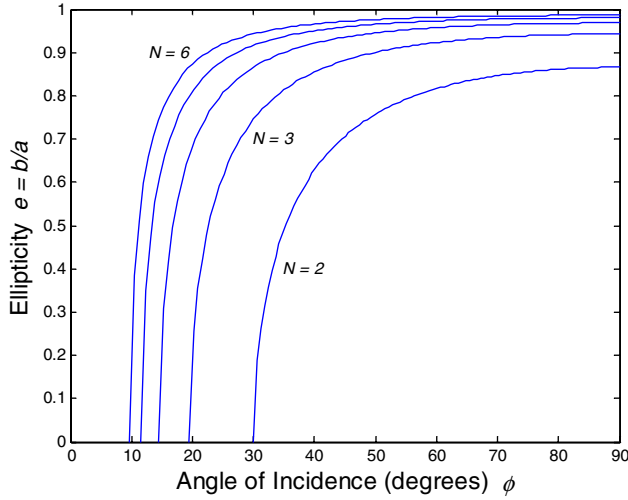
Fig. 3. (Color online) Ellipticity $e = b/a$ of the evanescent electric field [Eq. (10)] is plotted as a function of ϕ from the critical angle to grazing incidence at constant values of N from 2 to 6 in steps of 1.

Equation (12) indicates that $e_{\max} \geq 0.95$ is achieved if $N \geq 3.2026$.

As a specific example consider TIR at the GaP–air interface. GaP is transparent in the 620–760 nm red visible spectrum and also in the near- and middle-IR and has a refractive index of 3.3 at the He–Ne laser wavelength $\lambda = 633$ nm [11]. With $N = 3.3$, Eq. (11) gives $e_{\max} = 0.953$. And according to Eq. (10), e increases slightly from 0.950 at $\phi = 76.04°$ to $e_{\max} = 0.953$ at $\phi = 90°$. This confirms that ENCSs can be achieved in TIR at the GaP–air interface at incidence angles sufficiently below 90°.

As another example, consider TIR of IR radiation at the Ge–air interface for which $N \approx 4$ over a broad bandwidth [12]. Substitution of $N = 4$ in Eq. (11) gives $e_{\max} = \sqrt{15/16} = 0.968$. Equation (10) indicates that e increases from 0.950 at $\phi = 53.19°$ to $e_{\max} = 0.968$ at $\phi = 90°$. Once again this proves that ENCSs are realizable in TIR of IR radiation at the Ge–air interface at incidence angles well below 90°.

3. Circular Polarization of the Tangential Electric Field of the Evanescent Wave in the Plane of the Interface

For TIR of incident monochromatic light of arbitrary polarization,

$$\chi_i = E_{is}/E_{ip}, \tag{13}$$

the polarization state of the tangential (t) electric field of the evanescent wave in the plane of the interface is given by

$$\chi_{et} = E_{ez}/E_{ey}. \tag{14}$$

From Eqs. (1)–(4), (13), and (14) we obtain

$$\chi_{et} = (\cos\phi/\chi_i)[(r_p - 1)/(r_s + 1)]. \tag{15}$$

Circular polarization of the tangential field is achieved if

$$\chi_{et} = \pm j. \tag{16}$$

We take $\chi_{et} = +j$ and use Eqs. (5), (13), and (15) to obtain

$$\begin{aligned}
\chi_i &= E_{is}/E_{ip} \\
&= \cos\phi[\sin(\delta_p/2)/\cos(\delta_s/2)]\exp[j(\delta_p - \delta_s)/2].
\end{aligned} \tag{17}$$

Use of $\chi_{et} = -j$ instead of $\chi_{et} = +j$ simply changes the phase angle of the last term of Eq. (17) by π.

Equation (17) specifies the incident elliptical polarization state that causes the tangential electric field of the evanescent wave in the yz plane to be circularly polarized. From Eqs. (6) and (17) the required ratio of amplitudes of the s and p components of incident light is given by

$$\begin{aligned}
|\chi_i| &= |E_{is}|/|E_{ip}| \\
&= (N^2\sin^2\phi - 1)^{1/2}/[(N^2 + 1)\sin^2\phi - 1]^{1/2}, \tag{18}
\end{aligned}$$

and the associated phase difference is

$$\delta_{is} - \delta_{ip} = \arctan[(N^2\sin^2\phi - 1)^{1/2}/(N\sin\phi\tan\phi)]. \tag{19}$$

From Eq. (18) it is apparent that $|\chi_i| < 1$. Figure 4 shows $|\chi_i|$ plotted as a function of ϕ from the critical angle $\phi = \phi_c = \arcsin(1/N)$ to grazing incidence $\phi = 90°$ for constant values of N from 2 to 6 in steps of 1. Notice that $|\chi_i|$ initially rises steeply just above the critical angle and saturates at larger angles as
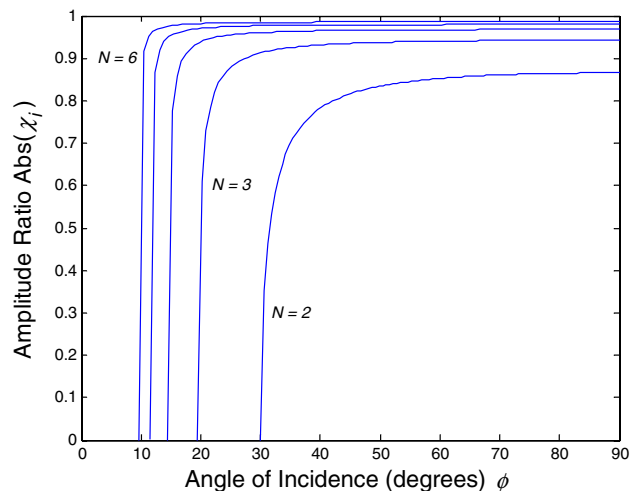

Fig. 4. (Color online) Amplitude ratio $|\chi_i| = E_{is}/E_{ip}$ [Eq. (18)] required to produce circular polarization of the tangential electric field in the plane of the interface is plotted as a function of ϕ from the critical angle to grazing incidence for constant values of N from 2 to 6 in steps of 1.

$\phi \to 90°$. From Eq. (18) the saturation value of $|\chi_i|$ at $\phi = 90°$ is given by

$$|\chi_i|_{90} = (N^2 - 1)^{1/2}/N. \tag{20}$$

Also of interest is $|\chi_i|$ at the angle of incidence $\phi_m = \arcsin\sqrt{2/(N^2 + 1)}$ at which the TIR differential phase shift $(\delta_p - \delta_s)$ is maximum [7]. At $\phi = \phi_m$, Eq. (18) simplifies to

$$|\chi_i| = (N^2 - 1)^{1/2}/(N^2 + 1)^{1/2}. \tag{21}$$

Figure 5 shows the amplitude ratios given by Eqs. (20) and (21) plotted versus N for $2 \leq N \leq 6$.

In Fig. 6, the phase difference between the incident s and p components at which the tangential electric field becomes circularly polarized [Eq. (19)] is plotted as a function of ϕ from the critical angle to grazing incidence for constant values of N from 2 to 6 in steps of 1.

Figures 4 and 6 indicate that to produce circular polarization ($\chi_{et} = +j$) of the tangential electric field in the plane of the boundary the incident polarization χ_i is limited to the first quadrant of the unit circle in the complex plane. A polarization state generator, e.g., a combination of a linear polarizer and a quarter-wave retarder, is used to polarize the incident light in any desired state [6].

4. Circular Polarization of the Transverse Electric Field of the Evanescent Wave

The polarization of the transverse (T) electric field of the z-traveling evanescent wave in the xy plane is given by

$$\chi_{eT} = E_{ey}/E_{ex}. \tag{22}$$

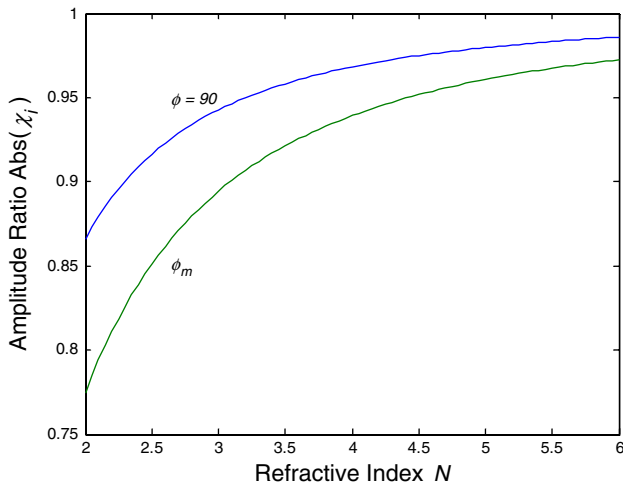
Fig. 5. (Color online) Amplitude ratio $|\chi_i| = E_{is}/E_{ip}$ for circular polarization of the tangential electric field at $\phi = 90°$ and $\phi_m = \arcsin\sqrt{2/(N^2 + 1)}$ [Eqs. (20) and (21)] is plotted versus N in the range $2 \leq N \leq 6$.
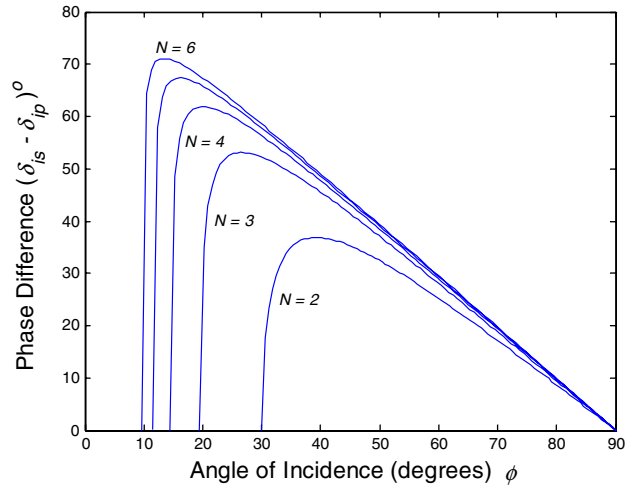

Fig. 6. (Color online) Phase difference $\delta_{is} - \delta_{ip}$ [Eq. (19)] between the incident s and p components of incident light, which is required to produce circular polarization of the tangential electric field, is plotted as a function of ϕ from the critical angle to grazing incidence for constant N values from 2 to 6 in steps of 1.

From Eqs. (1)–(4), (13), and (22) we obtain

$$\chi_i = \chi_{eT}(N^2 \sin\phi)[(r_p + 1)/(r_s + 1)]. \tag{23}$$

Circular polarization of the transverse field is achieved when $\chi_{eT} = \pm j$. We take $\chi_{eT} = +j$ and follow steps similar to those used in Section 3 to obtain

$$|\chi_i| = |E_{is}|/|E_{ip}| = (N\sin\phi)/[(N^2 + 1)\sin^2\phi - 1]^{1/2}, \tag{24}$$

$$\delta_{is} - \delta_{ip} = \arctan[(N^2\sin^2\phi - 1)^{1/2}/(N\sin\phi\tan\phi)] + \pi/2. \tag{25}$$

If $\chi_{eT} = -j$ is selected instead of $\chi_{eT} = +j$ the rightmost term of Eq. (25) changes from $+\pi/2$ to $-\pi/2$. Equation (25) differs from Eq. (19) only in the $+\pi/2$ added term.

Figure 7 shows $|\chi_i|$ of Eq. (24) plotted as a function of ϕ from the critical angle to grazing incidence at constant values of N from 2 to 6 in steps of 1. Note that $|\chi_i| > 1$ for all values of N and ϕ and that the limiting values of $|\chi_i|$ at ϕ_c and 90° are N and 1, respectively. For $\chi_{eT} = +j$, χ_i occupies the region of the second quadrant of the complex plane outside the unit circle.

5. Summary

Near-circular polarization of the evanescent field present in the rarer medium under conditions of TIR of incident p-polarized light at a dielectric–dielectric planar interface is achieved with high-index (>3.2) transparent prism materials (e.g., GaP and Ge) and at angles of incidence well above the critical angle but sufficiently below grazing incidence. Elliptical polarization of incident light with
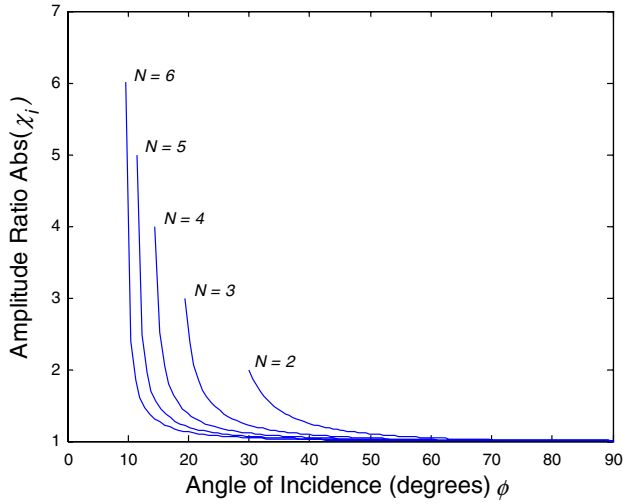
Fig. 7. (Color online) Amplitude ratio $|\chi_i| = E_{is}/E_{ip}$ [Eq. (24)], which is required to produce circular polarization of the transverse electric field of the evanescent wave, is plotted as a function of ϕ from the critical angle to grazing incidence for N values from 2 to 6 in steps of 1.

nonzero p and s components can be selected to produce circular polarization of the resultant tangential electric field in the plane of the interface or circular polarization of the transverse electric field in a plane normal to the direction of propagation of the evanescent wave. Control of the polarization of the evanescent light field in TIR influences its interaction with oriented molecules adsorbed at solid–liquid and solid–gas interfaces via the dot and cross products of the optical electric field with the electric dipole moments of such molecules [13].

Appendix A

The complex wave vector of the evanescent refracted plane wave in the Cartesian coordinate system of Fig. 1 is given by

$$\vec{k}_e = -jk_{ex}\hat{x} + k_{ez}\hat{z}, \qquad (A1)$$

and $\hat{x}$, $\hat{z}$ are unit vectors along the positive x and z axes. Phase matching across the boundary requires that the z components of the incident and refracted wave vectors be equal, i.e.,

$$k_{ez} = k_{iz} = (2\pi n_0/\lambda)\sin\phi, \qquad (A2)$$

where λ is the vacuum wavelength of light. We also have

$$\vec{k}_e \cdot \vec{k}_e = (2\pi n_1/\lambda)^2 = k_{ez}^2 - k_{ex}^2. \qquad (A3)$$

From Eqs. (A2) and (A3)

$$k_{ex} = (2\pi n_1/\lambda)(N^2\sin^2\phi - 1)^{1/2} \qquad (A4)$$

is obtained, where $N = n_0/n_1$.

For incident p-polarized light the evanescent wave field is given by

$$\vec{E}_e(x,y,z) = [\,E_{ex} \quad 0 \quad E_{ez}\,]^t \exp(-k_{ex}x)\exp(-jk_{ez}z). \qquad (A5)$$

In the absence of free charge in the medium of refraction, the wave field of Eq. (A5) must satisfy Gauss's law

$$\nabla \cdot \vec{E}_e = 0. \qquad (A6)$$

Setting the divergence of the right-hand side of Eq. (A5) equal to zero leads to

$$\chi_e = E_{ez}/E_{ex} = jk_{ex}/k_{ez}. \qquad (A7)$$

If k_{ez} and k_{ex} of Eqs. (A2) and (A4) are substituted in Eq. (A7) we obtain

$$\chi_e = j[1 - (\csc\phi/N)^2]^{1/2}, \qquad (A8)$$

in agreement with Eq. (10).

References

1. F. de Fornel, *Evanescent Waves* (Springer, 2001).
2. L. Novotny and B. Hecht, *Principles of Nano-Optics* (Cambridge, 2006).
3. L. Józefowski, J. Fiutowski, T. Kawalec, and H.-G. Rubahn, "Direct measurement of the evanescent-wave polarization state," J. Opt. Soc. Am. B **24**, 624–628 (2007).
4. A. Norrman, T. Setälä, and A. T. Friberg, "Partial coherence and partial polarization in random evanescent fields on lossless interfaces," J. Opt. Soc. Am. A **28**, 391–400 (2011).
5. R. H. Muller, "Definitions and conventions in ellipsometry," Surf. Sci. **16**, 14–33 (1969).
6. R. M. A. Azzam and N. M. Bashara, *Ellipsometry and Polarized Light* (North-Holland, 1987).
7. R. M. A. Azzam, "Phase shifts that accompany total internal reflection at a dielectric-dielectric interface," J. Opt. Soc. Am. A **21**, 1559–1563 (2004).
8. E. H. Hellen, R. M. Fulbright, and D. Axelrod, "Total internal reflection fluorescence theory and applications at biosurfaces," in *Spectroscopic Membrane Probes*, L. M. Loew, ed. (CRC Press, 1988), Vol. II, pp. 47–79.
9. K. H. Drexhage, "Interaction of light with monomolecular dye layers," in *Progress in Optics*, E. Wolf, ed. (Elsevier, 1974), Vol. 12, pp. 163–232.
10. S. E. Sund, J. A. Swanson, and D. Axelrod, "Cell membrane orientation visualized by polarized total internal reflection fluorescence," Biophys. J. **77**, 2266–2283 (1999).
11. A. Borghesi and G. Guizzetti, "Gallium phosphide," in *Handbook of Optical Constants of Solids*, E. D. Palik, ed. (Academic, 1985), pp. 445–464.
12. W. J. Tropf, M. E. Thomas, and T. J. Harris, "Properties of crystals and glasses," in *Handbook of Optics*, M. Bass, ed. (McGraw-Hill, 1995), Vol. I, Chap. 33.
13. J. Michl and E. W. Thulstrup, *Spectroscopy with Polarized Light* (VCH, 1995).